Targeting angiogenesis as a therapeutic means to reinforce osteocyte survival and prevent nonunions in the aftermath of radiotherapy

Alexis Donneys, MD, MS,[1] Noah S. Nelson, BS,[1] Erin E. Page,[1] Sagar S. Deshpande, BS,[1] Peter A. Felice, MD,[1,2] Catherine N. Tchanque–Fossuo, MD, MS,[1] Joshua P. Spiegel,[1] Steven R. Buchman, MD[1]*

[1]Craniofacial Research Laboratory, Plastic Surgery Section, University of Michigan, Ann Arbor, Michigan, [2]Department of General Surgery, University of South Carolina School of Medicine, Columbia, South Carolina.

Accepted 3 May 2014
Published online 10 July 2014 in Wiley Online Library (wileyonlinelibrary.com). DOI 10.1002/hed.23744

ABSTRACT: *Background.* Radiotherapy (XRT) exerts detrimental collateral effects on bone tissue through mechanisms of vascular damage and impediments to osteocytes, ultimately predisposing patients to the debilitating problems of late pathologic fractures and nonunions. We posit that angiogenic therapy will reverse these pathologic effects in a rat model of radiated fracture healing.

Methods. Three groups of rats underwent mandibular osteotomy. Radiated groups received a fractionated 35-Gy dose before surgery. The deferoxamine (DFO) group received local injections postoperatively. A 40-day healing period was allowed before histology. Analysis of variance (ANOVA; $p < .05$) was used for group comparisons.

Results. Radiated fractures revealed a significantly decreased osteocyte count and corresponding increase in empty lacunae when compared to nonradiated fractures ($p = .001$). With the addition of DFO, these differences were not appreciated. Further, a 42% increase in bony unions was observed after DFO therapy.

Conclusion. Targeting angiogenesis is a useful means for promoting osteocyte survival and preventing bone pathology after XRT. © 2014 Wiley Periodicals, Inc. *Head Neck* **37:** 1261–1267, 2015

KEY WORDS: deferoxamine, radiation, mandible, angiogenesis, nonunion

INTRODUCTION

Over 53,000 men and women were diagnosed with head and neck cancers and an additional 11,000 patients died from complications relating to these cancers in 2012.[1] Radiation therapy (XRT) is a standard adjuvant therapy for patients with head and neck cancer, and while the delivery of this treatment has become more precise with the development of intensity-modulated XRT,[2,3] the pernicious effects of XRT on normal, healthy tissues remains a concern. The population of cancer survivors who develop osteoradionecrosis (ORN), pathologic fractures, and subsequent nonunions after XRT experience a diminished quality of life. Their ability to eat, drink, speak, and socialize may be enormously impacted by the deleterious side effects of this necessary but destructive therapy. Frequently, ORN is a late finding and inciting event to pathologic fractures and associated nonunions. A therapeutic means designed to prevent this progression would therefore be highly desirable.

Deferoxamine (DFO) is a widely utilized iron chelator, currently on formulary for the treatment of iron toxicity.[4] DFO is generally well-tolerated, with only minor side effects, such as mild nausea and discomfort.[5–7] In addition to the utility of DFO as an iron chelator, it has also demonstrated the potential to upregulate angiogenesis via the stimulation of the hypoxia-inducible factor-1-alpha pathway. When given in minute, localized intermittent doses, DFO induces vascular endothelial growth factor production, in addition to other mediators of angiogenesis, resulting in the augmentation of resident vasculature and the production of new blood vessels.[8] Furthermore, investigators have recently demonstrated that triggering an upregulation of vascular endothelial growth factor directly stimulates osteogenesis, at comparable levels to bone morphogenic protein 2 in vivo.[9–12]

Although the majority of DFO research has been in the context of long bone animal models, previous work in our laboratory has demonstrated the ability of DFO to augment the vascular networks of irradiated mandibles after fracture repair.[13,14] The purpose of this project was to examine the ability of DFO to replenish the cellular environment of these irradiated mandibles through the metrics of histologic analysis. We posit that DFO will increase bone cellularity and ameliorate osteocyte function, leading to a marked improvement in overall bone healing after XRT.

***Corresponding author:** S. R. Buchman, University of Michigan Medical School, Pediatric Plastic Surgery Section, 4-730 C. S. Mott Children's Hospital, 1540 E. Hospital Drive, Ann Arbor, MI 48109-4215. E-mail: sbuchman@med.umich.edu

Contract grant sponsor: Funding supported by the following grants from the National Institutes of Health: "Translational Optimization of Bone Regeneration in the Irradiated Mandible" (CA12587-06) to Steven R. Buchman; "Training Grant in Trauma, Burn, and Wound Healing Research" (T32-GM008616) for Alexis Donneys; and The Plastic Surgery Foundation Pilot Award to Alexis Donneys for proposal titled "Therapeutic Prevention of Radiation Induced Non-Unions."

MATERIALS AND METHODS

Experimental design

Animal experimentation was performed in compliance with the guidelines published in the *Guide for the Care and Use of Laboratory Animals: Eighth Edition*, ISBN-10: 0-309-15396-4. Our protocols were approved by the University of Michigan's Committee for the Utilization and Care of Animals before implementation. Thirty-five adult male Sprague Dawley rats (400 g) were paired in cages in a specific pathogen-free vivarium and maintained on a 12-hour light/dark cycle. Before irradiation, the rats had a 7-day acclimation period. The animals were randomly assigned into 3 groups, each undergoing fracture repair. Group 1 ($n = 11$; Fx) served as our control fracture repair group, undergoing only the osteotomy. Group 2 ($n = 12$; XFx) received XRT 2 weeks before the osteotomy surgery. Group 3 ($n = 12$; XFxDFO) received XRT, underwent osteotomy surgery 2 weeks later, and was then administered DFO treatment.

Irradiation protocol

All radiation was performed in the Irradiation Core in the University of Michigan Department of Radiation Oncology. After induction of anesthesia via an oxygen/isoflurane mixture, left hemimandibles were irradiated using a Philips RT250 orthovoltage unit (250 kV X-rays, 15 mA; Kimtron Medical, Woodbury, CT). The animals were administered ionizing radiation through a filtered system to our specific region of interest (ROI), which spans a 2 mm distance posterior to the third molar, corresponding to the future site of the osteotomy. Localized delivery was ensured by using a lead shield placed over the rat exposing only our ROI. A human-equivalent dose of radiation, developed with the guidance of the Department of Radiation Oncology, was utilized. A fractionated dose of 7 Gy per day was administered over 5 days for a total of 35 Gy. This is equivalent to 70 Gy in human mandibular high-dose XRT, which was used to predictably replicate the pathologies similar to those seen in the setting of clinically advanced mandibular ORN.[15–17]

Perioperative care

Rats were administered gentamicin (5 mg/kg SQ) once before surgery and twice postoperatively. For analgesia, rats were administered buprenorphine (0.03 mg/kg SQ) in lactated Ringer's solution (25 mL/kg). Animals were anesthetized using an oxygen-isoflurane mixture. Postoperatively, animals were administered buprenorphine twice daily through postoperative day 5, and as needed thereafter. Weight gain, porphyrin staining, and fluid intake were monitored to determine the need for continued analgesia.

Surgical procedure

After sterile preparation and draping, a 2 cm midline incision was placed ventrally from the anterior submentum to the neck crease. An external fixator device was placed and secured, as previously described in the literature.[18] A vertical osteotomy was performed directly behind the third molar of the left hemimandible using a reciprocating saw blade. A fixed 2 mm fracture gap was set 4 hours postoperatively by turning the fixator screw clockwise a total of 7 times. This gap ensures a grossly visible separation that can be later sectioned and analyzed histologically. After a 40-day healing period, the animals were euthanized and left hemimandibles were harvested for union analysis and histologic processing. Union was defined as gross bony bridging with the absence of motion across the fracture site after fixator removal. Of note, we experienced 1 fatality during the surgical procedure, resulting in the loss of 1 animal from the Fx group.

Deferoxamine dosing

The DFO-treated group was administered localized injections (200 μmol/300 μL) directly into the fracture site every other day from postoperative day 4 to 12 for a total of 5 doses. This time period was selected to coincide with the initiation of angiogenesis in a murine fracture model.[19]

Histologic processing

After the 40-day fracture healing period, the mandibles were fixed with 70% ethanol, and subsequently rinsed in phosphate-buffered saline. The samples were then decalcified using Cal-ExII (10.6% formic acid, 7.4% formaldehyde, <1% methyl alcohol; Fisher Scientific, Fair Lawn, NJ) and stored at 4°C. The solution was changed daily and total decalcification was confirmed radiographically using a self-contained Faxitron X-Ray device (MX20; Faxitron X-Ray, Lincolnshire, IL). The samples were vacuum processed (dehydration and paraffin infiltration) under a 48-hour program in a Hypercenter tissue processor (Hypercenter XP; Shandon, Pittsburg, PA), then filtrated once more for 2 hours in a vacuum bath. They were subsequently embedded in Paraplast Plus (McCormic Scientific; Richmond, IL) in 22- × 40-mm peel-away molds and stored overnight at 4°C. The blocks were sectioned coronally from anterior to posterior into 7-micron thick sections taken on a Leica Richert–Jung microtome (model 2030; Biocut, Bensheim, Germany), and mounted on glass slides. The sections were surface-stained with Gomori's trichrome.

Histomorphometric evaluation

In order to count the number of osteocytes and empty lacunae, we utilized a light microscope interfaced with a camera linked to a computer. Our ROI spanned a distance of 2 mm posterior to the third molar, encompassing the site of fracture repair. The ROI was superimposed on the digital image using Bioquant NOVA Osteo version 7 imaging analysis software (R&M Biometrics, Nashville, TN). Nine high-power-field images were selected at random for each ROI using 16× magnification. Three reviewers independently performed the point counting of osteocytes and empty lacunae.

Thresholding evaluation

Digital images of each slide were loaded onto the previously mentioned Bioquant software package in order to measure the tissue volume and osteoid volume of each sample. Mature bone stained blue and immature bone stained pink, allowing for easy distinction during the

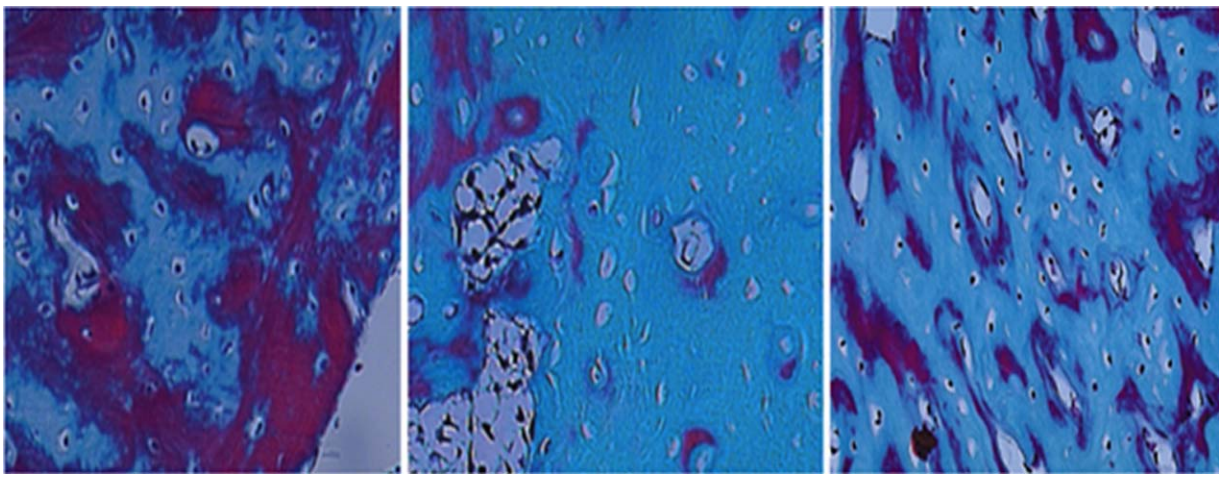

FIGURE 1. From left to right, fracture group (Fx), radiated group (XFx) and deferoxamine-treated group (XFxDFO). Digital photograph stained with Gomori's trichrome at 16× magnification demonstrating DFO-treated restoration of osteocyte count and osteoid (pink). Note the comparative depletion of osteocytes and increase in empty lacunae in the radiated group (center). [Color figure can be viewed in the online issue, which is available at wileyonlinelibrary.com.]

thresholding process. The software calculated the osteoid volume/tissue volume ratio, which indicates the percentage of nonmineralized, immature bone in our ROI.

Statistical analysis

All data is presented as the mean ± SD. Values were analyzed with a 1-way analysis of variance (ANOVA) using PSAW for Windows version 21.0 (SPSS, Chicago, IL). Significance was assigned as $p < .05$.

RESULTS

Histomorphometric analysis

As expected, histologic analysis revealed a significant decrement in osteocyte number in the radiated group as compared to the Fx group (29.76 ± 10.83 vs 69.48 ± 10.86; $p = .01$; see Figure 1). We also saw a significant restoration in osteocyte count from the radiated group to the DFO-treated group (29.76 ± 10.83 vs 66.24 ± 6.36; $p = .01$). Interestingly, DFO treatment also demonstrated no significant difference in osteocyte count from the Fx group (66.24 ± 6.36 vs 69.48 ± 10.86; $p = .67$), indicating a restoration to control level osteocyte viability (see Figure 2).

Similarly, further histologic analysis revealed a significant increase in empty lacunae number in the radiated group as compared to the Fx group (7.20 ± 3.86 vs 2.11 ± 0.98; $p = .002$; see Figure 3). The number of empty lacunae is a corroborating metric indicating osteocyte death; therefore, a decreased osteocyte count

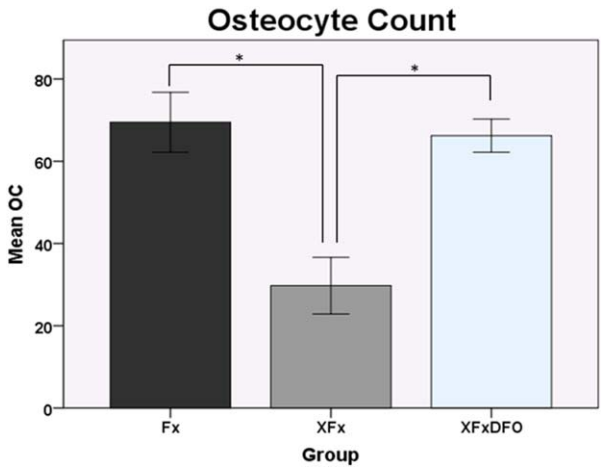

FIGURE 2. Osteocyte count per high power field means and SDs for the fracture group (Fx), radiated group (XFx), and deferoxamine-treated group (XFxDFO). *Denotes significance at $p < .05$ between means. [Color figure can be viewed in the online issue, which is available at wileyonlinelibrary.com.]

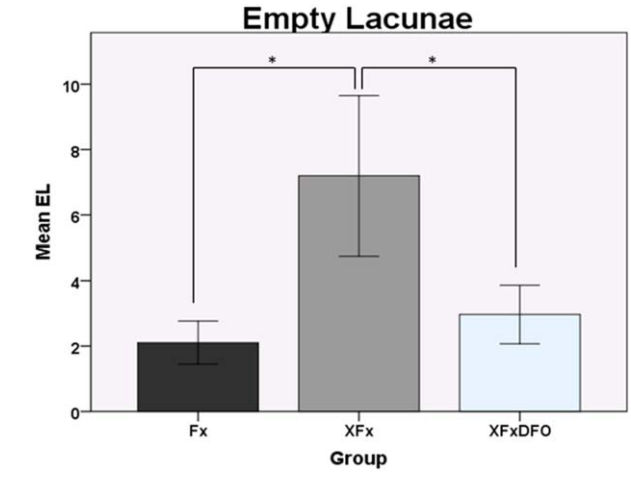

FIGURE 3. Empty lacunae count per high power field means and SDs for the fracture group (Fx), radiated group (XFx), and deferoxamine-treated group (XFxDFO). *Denotes significance at $p < .05$ between means. [Color figure can be viewed in the online issue, which is available at wileyonlinelibrary.com.]

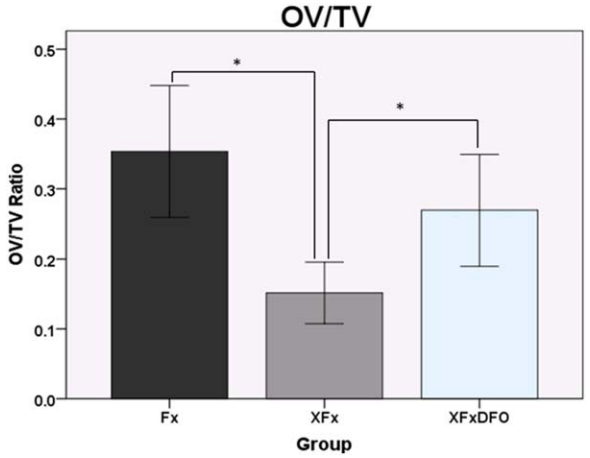

FIGURE 4. Ratio of nonmineralized, immature bone in the region of interest (ROI; osteoid volume/tissue volume) means and SDs for the fracture group (Fx), radiation group (XFx), and deferoxamine-treated group (XFxDFO). *Denotes significance at $p < .05$ between means. [Color figure can be viewed in the online issue, which is available at wileyonlinelibrary.com.]

typically correlates with an increase in empty lacunae, as seen in our XFx group. We also saw a corresponding significant decrease in empty lacunae when comparing XFx to XFxDFO (7.20 ± 3.86 vs 2.97 ± 1.41; $p = .008$). Again, DFO treatment decreased the number of empty lacunae to levels that were not significantly different from the Fx group (2.97 ± 1.41 vs 2.11 ± 0.98; $p = .23$), indicating a restoration to control levels.

Thresholding analysis

The osteoid volume/tissue volume in the ROI was found to be significantly lower in the XFx group when compared to the Fx group ($15.2\% \pm 6.9\%$ vs $35.4\% \pm 14.1\%$; $p = .001$; see Figure 4). Treatment with DFO showed a significant improvement in the osteoid volume/tissue volume ratio as compared to the XFx group ($26.9\% \pm 12.6\%$ vs $15.2\% \pm 6.9\%$; $p = .045$). In accordance with our hypothesis, the osteoid volume/tissue volume ratio for the group treated with DFO was not significantly different from the Fx group ($35.4\% \pm 14.1\%$ vs $26.9\% \pm 12.6\%$; $p = .203$), indicating a restoration to control levels (see Figure 1).

Bony union

After a 40-day recovery period, the Fx mandibles demonstrated complete bony union in 100% (all of 11) of specimens, as expected. With the addition of XRT, XFx mandibles only exhibited a 25% (3 of 12) union rate. The treatment of radiated fractures with DFO increased the rate of bony union to 67%, (8 of 12), indicating a marked improvement from the XFx group.

Qualitative assessments

We observed decreased hematopoietic cellularity (see Figure 5) and periosteal fibrosis and detachment, consistent (see Figure 6) with radiation damage in our XFx group. These changes were not observed in the XFxDFO group, indicating a preservation of hematopoietic cellularity and periosteal attachment. In addition, nuclear changes, such as karyolysis (fading), pyknosis (shrinkage), and karyorrhexis (fragmentation) were seen in the XFx group (see Figure 7). These changes were visibly reduced in the XFxDFO group, indicating a preservation of nuclear integrity.

DISCUSSION

The effects of XRT on bone tissue are often not appreciated until cumulative tissue damage leads to functional and mechanical failures requiring surgical intervention. Ascertaining the optimal time point when tumor recurrence is minimal and mechanical failure has not yet

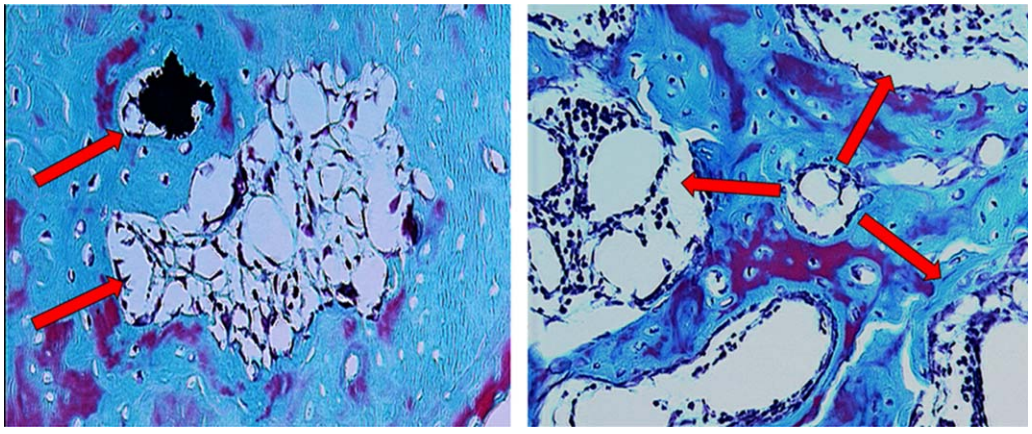

FIGURE 5. Digital photograph stained with Gomori's trichrome at 16× magnification demonstrating clotting, cellular fibrosis, and depletion of cellularity in the hematopoietic cavities observed in the radiation group (XFx) group (left), which is not evident in the deferoxamine-treated group (XFxDFO) specimen (right). Note the marrow cavities teeming with viable, robust hematopoietic cells in the DFO-treated mandibles in contradistinction. [Color figure can be viewed in the online issue, which is available at wileyonlinelibrary.com.]

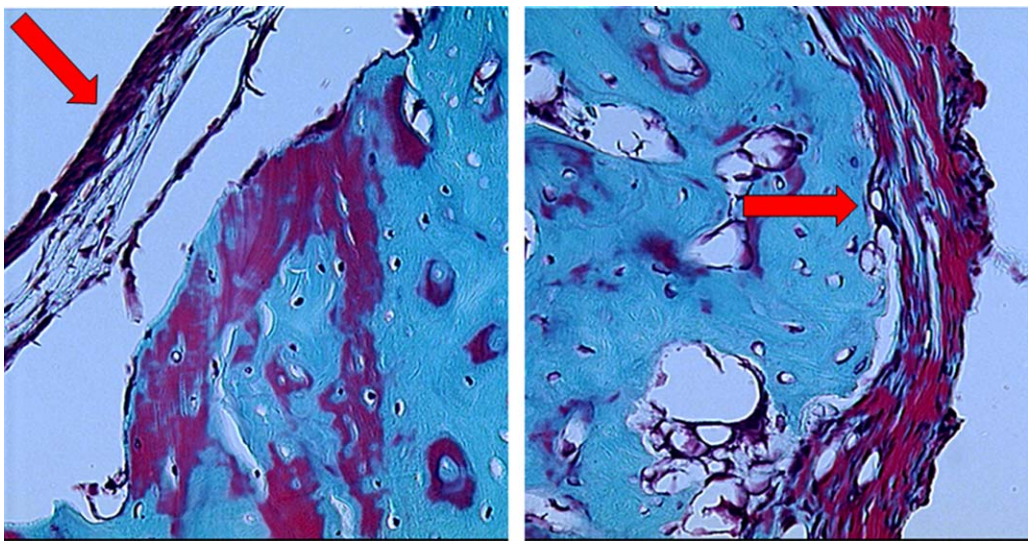

FIGURE 6. Digital photograph stained with Gomori's trichrome at 16× magnification demonstrating periosteal fibrosis and detachment in the radiation group (XFx) group (left), which is not evident in the deferoxamine-treated group (XFxDFO) specimen (right). [Color figure can be viewed in the online issue, which is available at wileyonlinelibrary.com.]

ensued would serve as a window of opportunity for therapies designed to reverse the underlying effects of radiation on bone. We have previously established a rat model of pathologic fracture healing after XRT whereby nonunions consistently developed in 75% to 80% of cases.[13,14] Admittedly, this model does not take into account any oncologic incidence or progression; however, it does give us a platform whereby we can examine and quantify mechanical failure in the form of failed bony union in response to the aberrant effects of radiation on bone healing. Previous work in our laboratory has quantifiably demonstrated the ability of DFO to augment the vascularity, mineralization, and mechanical strength of fracture healing in this model, and this communication

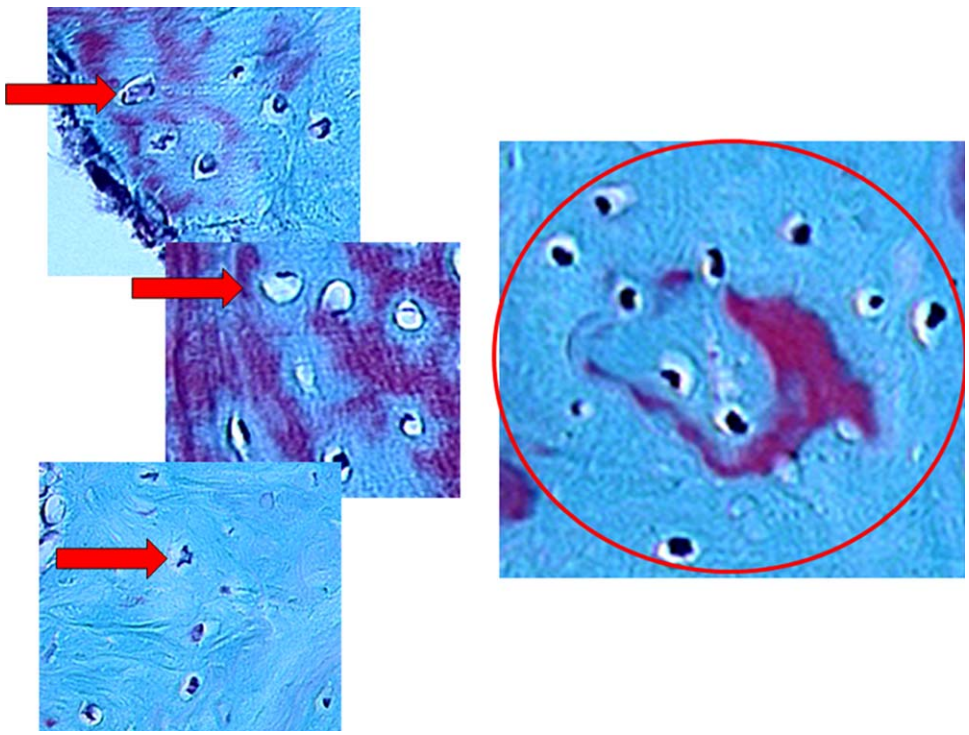

FIGURE 7. Digital photograph stained with Gomori's trichrome at 16× magnification demonstrating nuclear fading (upper left arrow), shrinkage (middle left arrow), and fragmentation (bottom left arrow) in the radiation group (XFx) group. The deferoxamine-treated group (XFxDFO) group (right) contains robust nuclei in the osteocytes. [Color figure can be viewed in the online issue, which is available at wileyonlinelibrary.com.]

specifically examines the effect of osteocyte survival and function within this context.

In this study, we observed significant quantifiable depletions in histologic metrics after radiated fracture healing that were restored to control levels with the addition of DFO therapy. In particular, DFO demonstrated the capability to produce significantly higher osteocyte counts and lower empty lacunae levels than the XFx group. In addition, osteocyte counts and empty lacunae values were not significantly different from Fx controls, suggesting that DFO has the ability to restore cellularity to levels expected during normal fracture healing in nonradiated bone.

Histologically, osteoid is the unmineralized, organic portion of bone matrix. Osteoid is formed by functional osteoblasts before subsequent mineralization and succession to mature bone tissue. Our thresholding analysis revealed a severe restriction in the ability of radiated bone to produce osteoid. This effect was not observed in DFO-treated mandibles. In fact, DFO-treated mandibles exhibited osteoid volume/tissue volume ratios that were not statistically different than control, supporting our hypothesis that an indirect effect on therapeutic vascular augmentation played a critical role in restoring early bone production. Qualitative findings also afforded unique insights into the overall histologic effects of DFO in preventing radiation-induced damage. We observed structural damage consisting of hematopoietic cell depletion, periosteal fibrosis and detachment, and nuclear changes because of XRT that were not evident in DFO-treated mandibles.

Ultimately, these findings amalgamated to a clinically relevant increase in the rate of bony union, as DFO-treated mandibles exhibited a 2.5-fold increase in the rate of bone union despite exposure to XRT.

Undoubtedly, using an angiogenic therapeutic strategy in an area of previous malignancy raises concerns. Some authors have even suggested the utility of antiangiogenic agents as antitumor treatments.[20,21] However, although we did not take into account the tumorigenicity of DFO, there is evidence that DFO may, in fact, have antitumorigenic properties. Studies by Kulp et al[22] and Hann et al[23] suggest that DFO promotes apoptosis and decreased survival in p53+ tumor cells, as well as deprives hepatocellular carcinoma cells of the iron stores necessary for DNA replication. Further, Lee et al[24,25] report evidence demonstrating the antitumorigenic effect of DFO in in vitro studies of oral keratinocytes. His studies suggest growth arrest and cytochrome c-dependent apoptosis in immortalized and malignant oral keratinocytes. Although our studies are not particularly concerned with the possibility of treating oral cancers with DFO, their studies lend important evidence for suggesting the potentially safe and efficacious use of DFO at a remote time from oncologic management.

Taken together, we support the continued investigation of this promising therapy for its potential optimization and use in the head and neck cancer population for the prevention and treatment of pathologic fractures and nonunions because of XRT. Further, we argue that the surgical removal of tumor, subsequent radiation, and the temporal distance from oncologic management to the timing of the development of bone pathologies favor the potential use of this therapy at a remote time from oncologic management that precedes the events of mechanical failure.

CONCLUSIONS

This study demonstrates that DFO replenishes osteocyte count, reverses tissue damage, and increases union rate after XRT in a model of mandibular pathologic fracture repair. Future directions include combining DFO therapy with radioprotectants or stem cell therapies to further delineate the optimum regimen to improve fracture site cellularity and healing. Because of its clinical applicability and outlet for future research, DFO is a promising option for the prevention and treatment of pathologic fractures and nonunions associated with XRT.

Acknowledgments

The authors thank Mary Davis and Dave Karnak for assistance with the delivery of XRT and Charles Roehm for fixator device fabrication.

REFERENCES

1. .American Cancer Society. Cancer Facts and Figures 2013. Available at: http://www.cancer.org/research/cancerfactsfigures/cancerfactsfigures/cancer-facts-figures-2013. Accessed January 1, 2014.
2. Cohen EE, Lingen MW, Vokes EE. The expanding role of systemic therapy in head and neck cancer. *J Clin Oncol* 2004;22:1743–1752.
3. Yang ES, Murphy BM, Chung CH, et al. Evolution of clinical trials in head and neck cancer. *Crit Rev Oncol Hematol* 2009;71:29–42.
4. Farberg AS, Jing XL, Monson LA, et al. Deferoxamine reverses radiation induced hypovascularity during bone regeneration and repair in the murine mandible. *Bone* 2012;50:1184–1187.
5. Karnon JK. Tolley JO, Oyee J, Jewitt K, Ossa D, Akehurst R. *Cost-utility analysis of deferasirox compared to standard therapy with desferrioxamine for patients requiring iron chelation therapy in the United Kingdom. Curr Med Res Opin* 2008;24:1609–1621.
6. Alymara V, Bourantas D, Chaidos A, et al. Effectiveness and safety of combined iron-chelation therapy with deferoxamine and deferiprone. *Hematol J* 2004;5:475–479.
7. Piga A, Galanello R, Forni GL, et al. Randomized phase II trial of deferasirox (Exjade, ICL670), a once-daily, orally-administered iron chelator, in comparison to deferoxamine in thalassemia patients with transfusional iron overload. *Haematologica* 2006;91:873–880.
8. Shen X, Wan C, Ramaswamy G, et al. Prolyl hydroxylase inhibitors increase neoangiogenesis and callus formation following femur fracture in mice. *J Orthop Res* 2009;27:1298–1305.
9. Behr B, Sorkin M, Lehnhardt M, Renda A, Longaker MT, Quarto N. A comparative analysis of the osteogenic effects of BMP-2, FGF-2, and VEGFA in a calvarial defect model. *Tissue Eng Part A* 2012;18:1079–1086.
10. Schmitt C, Lutz R, Doering H, Lell M, Ratky J, Schlegel KA. Bio-Oss® blocks combined with BMP-2 and VEGF for the regeneration of bony defects and vertical augmentation. *Clin Oral Implants Res* 2013;24:450–460.
11. Street J, Bao M, deGuzman L, et al. Vascular endothelial growth factor stimulates bone repair by promoting angiogenesis and bone turnover. *Proc Natl Acad Sci U S A* 2002;99:9656–9661.
12. Wan C, Gilbert SR, Wang Y, et al. Activation of the hypoxia- inducible factor-1alpha pathway accelerates bone regeneration. *Proc Natl Acad Sci U S A* 2008;105:686–691.
13. Donneys A, Weiss DM, Deshpande SS, et al. Localized deferoxamine injection augments vascularity and improves bony union in pathologic fracture healing after radiotherapy. *Bone* 2013;52:318–325.
14. Donneys A, Deshpande SS, Tchanque–Fossuo CN, et al. Deferoxamine expedites consolidation during mandibular distraction osteogenesis. *Bone* 2013;55:384–390.
15. Tchanque–Fossuo CN, Monson LA, Farberg AS, et al. Dose-response effect of human equivalent radiation in the murine mandible: part I. *A histomorphometric assessment. Plast Reconstr Surg* 2011;128:114–121.
16. Tchanque–Fossuo CN, Monson LA, Farberg AS, et al. Dose-response effect of human equivalent radiation in the murine mandible: part II. *A biomechanical assessment. Plast Reconstr Surg* 2011;128:480e–487e.
17. Monson LA, Farberg A, Jing L, Buchman SR. Human equivalent radiation dose response in the rat mandible. *Plast Reconstr Surg* 2009;124:2.
18. Buchman SR, Ignelzi MA Jr, Radu C, et al. Unique rodent model of distraction osteogenesis of the mandible. *Ann Plast Surg* 2002;49: 511–519.

19. Glowacki J. Angiogenesis in fracture repair. *Clin Orthop Relat Res* 1998; (355 Suppl):S82–S89.
20. Abdollahi A, Folkman J. Evading tumor evasion: current concepts and perspectives of anti-angiogenic cancer therapy. *Drug Resist Updat* 2010;13:16–28.
21. Tugues S, Koch S, Gualandi L, Li X, Claesson–Welsh L. Vascular endothelial growth factors and receptors: anti-angiogenic therapy in the treatment of cancer. *Mol Aspects Med* 2011;32:88–111.
22. Kulp KS, Vulliet PR. Mimosine blocks cell cycle progression by chelating iron in asynchronous human breast cancer cells. *Toxicol Appl Pharmacol* 1996;139:356–364.
23. Hann HW, Stahlhut MW, Rubin R, Maddrey WC. Antitumor effect of deferoxamine in human hepatocellular carcinoma growing in athymic nude mice. *Cancer* 1992;70:2051–2056.
24. Lee SK, Lee JJ, Lee HJ, et al. Iron chelator-induced growth arrest and cytochrome c-dependent apoptosis in immortalized and malignant oral keratinocytes. *J Oral Pathol Med* 2006;35:218–226.
25. Lee SK, Jang HJ, Lee HJ, et al. p38 and ERK MAP kinase mediates iron chelator-induced apoptosis and -suppressed differentiation of immortalized and malignant human oral keratinocytes. *Life Sci* 2006;79:1419–1427.